

Detailed Study of a Molecule in a Molecule: N-Acetyl-L-tryptophanamide in an Active Site Model of α -Chymotrypsin

G. Dive,* D. Dehareng, and J. M. Ghuysen

Contribution from the Center for Protein Engineering, University of Liège, Institut de Chimie, B6, B-4000 Sart Tilman, Liège 1, Belgium

Received October 4, 1993. Revised Manuscript Received December 1, 1993*

Abstract: Six complexes between a model active site of α -chymotrypsin (261 atoms) and N-acetyl-L-tryptophanamide (33 atoms) were optimized at the semiempirical AM1 level. In one of these complexes, a water molecule was included. A detailed study at the geometric and energetic levels is presented. The discussion deals with the nature of the interaction, the effect of the environment, the ligand deformation, the backbone relaxation, the water molecule freedom, and the comparison with the molecular mechanics results.

Introduction

The serine proteases have been the matter of a great number of studies for many years. They owe their denominations to the existence of a conserved serine that acts as a nucleophile toward their substrates. Moreover, the existence of a conserved triad Ser-His-Asp was pointed out by Blow et al.¹ that could be subject to a proton transfer, be it modeled as double¹ or simple.²⁻⁵

Theoretical investigations of this proton transfer^{5,6} or of the enzymatic mechanisms⁷⁻¹⁰ were done on models at the quantum chemistry level, and dynamic studies were performed namely on acyl enzymes of chymotrypsin at the molecular mechanics level.^{11,12}

Theoretical reviews about enzymatic reactions were published by Kollman¹³ and Warshel,¹⁴ and an interesting historical overview on serine proteases can be found in the introduction of the article by Nakagawa et al.¹¹

A detailed analysis of the Michaelis complex and the tetrahedral intermediate was made for several conformations of the L and D configurations of N-acetyltryptophanamide in a model active site of α -chymotrypsin¹⁵ to study the stereoselectivity of the enzyme. This work will serve as a reference for the present contribution.

The aim of our work is not at all to focus on the mechanistic approach but to analyze in detail a particular complex of a molecule (the ligand N-acetyl-L-tryptophanamide, hereafter noted TRYPT) in a molecule [the α -chymotrypsin active site model,

noted CHT(23) in the following] at the geometric and energetic points of view at a quantum chemistry level.

To our knowledge, it is the first time that calculations at the quantum chemistry level have been performed on such large molecular systems. Our results are compared with those obtained at the molecular mechanics¹⁵ and electrostatic energy levels.

The nature of the interaction, the influence of the interacting residues' environment, the ligand deformation, and backbone relaxation are discussed for six optimized complexes, one of which includes a water molecule.

Four links of GAUSSIAN86¹⁶ were adapted to deal with large molecules (about 350 atoms and 1000 AO).

Used To Gather Information

All the optimizations and single-point AM1 calculations were done with GAUSSIAN86 on a FPS264 processor (38 Mflops) attached to a Digital Vax-4200.

The *ab initio* single-point calculations were done with a "home-adapted" UNIX version of GAUSSIAN92¹⁷ on a FPS511EA.

The energy decompositions were done with program G80 from AMBER.¹⁸

The links 103, 401, 402, and 716 of GAUSSIAN86 were modified in order to handle very big molecular systems with a large number of internal variables to be optimized within a central memory of 32 Megabytes.

In the case of the CHT(23) + TRYPT complex, the time needed for one calculation of the energy and the forces is about 3.5 h.

Modification of Link 103. The maximum number of steps taken into account in the memory allocation is no longer a function of the variable number but is set to the maximum number of optimization cycles introduced by the user.

Furthermore, according to the correction proposed by Dr. G. Lennes (private communication), a scalar product had to be multiplied by 2 in the deck DXLINR for the variables DGNOLD and DGNNEW.

Modification of Link 401. When introduced in the input stream, the external LCAO coefficients are no longer reorthogonalized and renormalized within the projected minimal basis set. This is useful for the first

* To whom correspondence should be sent: Telephone, +32-41-56.34.99; Fax +32-41-56.33.64.

• Abstract published in *Advance ACS Abstracts*, February 1, 1994.

(1) Blow, D. M.; Birktoft, J. J.; Harley, B. S. *Nature* 1969, 221, 337.
 (2) Wang, J. H. *Science* 1968, 161, 328.
 (3) Polgar, L.; Bender, M. L. *Proc. Natl. Acad. Sci. U.S.A.* 1969, 64, 1335.
 (4) Markley, J.; Ibanez, I. *Biochemistry* 1976, 15, 3399.
 (5) Kollman, P. A.; Hayes, D. M. *J. Am. Chem. Soc.* 1981, 103, 2955.
 (6) Stamato, F. M. L. G.; Longo, E.; Yoshioka, L. M. *J. Theor. Biol.* 1984, 107, 329.
 (7) Sheiner, S.; Lipscomb, W. N. *Proc. Natl. Acad. Sci. U.S.A.* 1976, 73, 432.
 (8) Stamato, F. M. L. G.; Tapia, O. *Int. J. Quantum Chem.* 1988, 33, 187.
 (9) Dive, G.; Peeters, D.; Leroy, G.; Ghuysen, J. M. *THEOCHEM* 1984, 107, 117.
 (10) Daggett, V.; Schroder, S.; Kollman, P. A. *J. Am. Chem. Soc.* 1991, 113, 8926.
 (11) Nakagawa, S.; Yu, H. A.; Karplus, M.; Umeyama, H. *Proteins* 1993, 16, 172.
 (12) Bemis, G. W.; Carlson-Golab, G.; Katzenellenbogen, J. A. *J. Am. Chem. Soc.* 1992, 114, 570.
 (13) Kollman, P. A. *Curr. Opin. Struct. Biol.* 1992, 2, 765.
 (14) Warshel, A. *Curr. Opin. Struct. Biol.* 1992, 2, 230.
 (15) Wipff, G.; Dearing, A.; Weiner, P. K.; Blaney, J. M.; Kollman, P. A. *J. Am. Chem. Soc.* 1983, 105, 997.

(16) GAUSSIAN86; Frisch, M. J.; Binkley, J. S.; Schlegel, H. B.; Raghavachari, K.; Melius, C. F.; Martin, R. L.; Stewart, J. J. P.; Bobrowicz, F. W.; Rohlfing, C. M.; Kahn, L. R.; Defrees, D. J.; Seeger, R.; Witherside, R. A.; Fox, D. J.; Fluder, E. M.; Topiol, S.; Pople, J. A. Carnegie-Mellon Quantum Chemistry Publishing Unit, Carnegie-Mellon University: Pittsburgh, PA 15213, 1986.

(17) GAUSSIAN92, Unix Revision B; Frisch, M. J.; Trucks, G. W.; Head-Gordon, M.; Gill, P. M. W.; Wong, M. W.; Foresman, J. B.; Johnson, B. G.; Schlegel, H. B.; Robb, M. A.; Replogle, E. S.; Gomperts, R.; Andres, J. L.; Raghavachari, K.; Binkley, J. S.; Gonzalez, C.; Martin, R. L.; Fox, D. J.; Defrees, D. J.; Baker, J.; Stewart, J. J. P.; Pople, J. A. Gaussian Inc., Carnegie-Mellon Quantum Chemistry Publishing Unit, Carnegie-Mellon University: Pittsburgh, PA 15213, 1992.

(18) AMBER; Singh, U. C.; Weiner, P. K.; Caldwell, J.; Kollman, P. A. University of California, San Francisco: 1986.

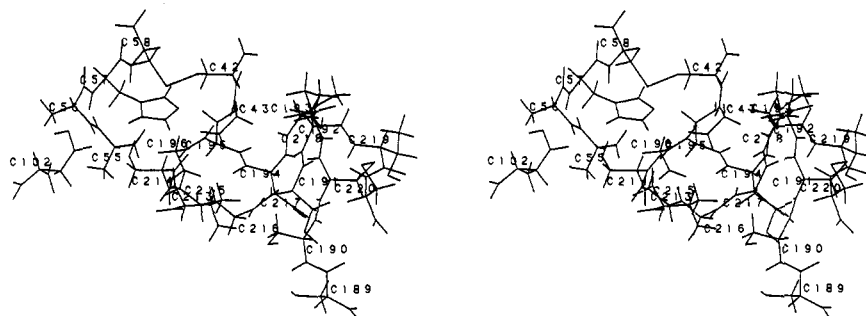


Figure 1. Stereoview of the CHT(23) optimized at the AM1 level according to the first optimization scheme (see text). The α carbons of every amino acid are indicated. The retained amino acids are the following: C42, G43, A55, A56, H57, C58, D102, S189, S190, C191, M192, G193, D194, S195, G196, V213, S214, G215, G216, S217, S218, T219, and C220.

run of the optimization if the LCAO coefficients are representative (for instance, CNDO coefficients for an AM1 run).

Furthermore, external LCAO coefficients and the related external overlap matrix that should be employed in the projection can be read on separate sequential files. This is useful for the subsequent optimization runs. For instance, the use of the last AM1 coefficients and overlap matrix of the run N can be used to begin the run $N + 1$ at the geometry of the run N . Then the first cycle is very fast.

Modification of Link 402. The external density matrix of run N can be read on a separate sequential file for run $N + 1$, as well as the LCAO coefficients and the overlap matrix.

The memory allocation for the β coefficients is suppressed (no UHF calculation possible any longer).

The α density matrix is considered alone and the total density matrix is dropped, thus providing some more memory availability.

The bielectronic integrals are no longer stored in the core but are written on a sequential file, by a packet of 128 000 words.

The core Hamiltonian H_{CORE} is also copied on a sequential file and is read when necessary.

The two extrapolation methods Pulay and Camp-King are suppressed, and only Extr34 is left. The first three SCF iterations are made with the complete diagonalization routine DiagD whereas all the other iterations use the rapid approximate routine Diag.

Modification of Link 716. After the routines FCINT and FXINT, the available memory was not reassigned. This has been changed in these two routines.

Furthermore, in the initialization of the link, 95% of the memory is allocated instead of 90%.

Building of the Model

The *N*-acetyl-L-tryptophanamide and α -chymotrypsin coordinates obtained by molecular mechanics energy refinement were kindly provided to us by Dr. G. Wipff.¹⁵

The construction of the active site model was realized in four steps.

The first three are described in ref 19. The three models CHT1, CHT2, and CHT3 presented therein consisted of respectively 6, 16, and 19 neutral amino acids taken from Wipff's coordinates of his LM1 complex.

Starting from CHT3, optimizations were performed on the active site, alone and including TRYPT as ligand (33 atoms, 87 atomic orbitals), within the semiempirical AM1²⁰ framework. In these calculations, all the side chains and all the ligand degrees of freedom were considered as variables but the NH-C α H-CO backbone was kept frozen. This optimization led, after 90 cycles, to the exclusion of TRYPT out of the enzyme cavity. As a matter of fact, the cavity was not correctly "closed" to handle the ligand in the pocket and a fourth model CHT(23) (261 atoms, 675 atomic orbitals) was constructed by adding to CHT3 the four residues Ser189, Ser217, Ser218, and Thr219 (Figure 1).

In this study, Asp102 and Asp194 were neutralized; otherwise it would have been necessary to introduce the neighboring

counterions in the calculation. Nevertheless, the H-bonds remain strong between Asp102 and His57 or Ser214.

For the CHT(23) molecule, only one AM1 energy minimization was performed, consisting of optimizing all the side chains' 222 internal coordinates while keeping the NH-C α H-CO backbone frozen. The nucleophilic serine Ser195 was oriented as in Wipff's LM1 model.

Three runs with a total of 84 cycles were done, leading to the optimized conformation with an AM1 heat of formation of -1.781 624 au. At the beginning of each run, a partial second derivative was calculated by finite differences, for the internal coordinates for which the first derivative was the highest.

For the CHT(23) + TRYPT molecular complex (294 atoms, 762 AO), five kinds of AM1 optimizations were performed. In each case, several runs were necessary to obtain a geometry at convergence. At the beginning of every run, the Hessian was numerically estimated for a reduced set of variables. A Hessian estimated in such a way provides reliable force constants for the chosen coordinates but is characterized by an incorrect inertia. As a matter of fact, the partial preset diagonal structure of the Hessian, corresponding to the variables for which no numerical calculation of the force constants is made, mixed with its correct diagonal and off-diagonal elements provides unrealistic negative eigenvalues (see Appendix). The variables for which the force constants were numerically estimated were chosen according to two criteria: first, they were those for which the component of the Hessian eigenvectors corresponding to the first two negative eigenvalues, in the preceding run, was higher than a given threshold; second, they were those for which the gradient component was higher than a chosen threshold.

The five kinds of AM1 optimizations were the following:

(1) Starting from Wipff et al.'s LM1 complex conformation, all the geometrical parameters of the CHT(23) side chains and of the TRYPT ligand were considered as variables but the NH-C α H-CO backbone was kept frozen. Thus, 342 internal coordinates were optimized. Nine runs with a total of 237 optimization cycles were done. The optimized complex is hereafter noted LM1 OPT. Its final AM1 heat of formation is -1.837 203 au, corresponding to a 53.48 kcal/mol stabilization from the starting geometry.

(2) Starting from LM1 OPT, the same 342 variables as in optimization 1 were optimized but the Ser195 side chain was rotated in such a way as to point its O γ toward the carbon of the TRYPT CO-NH scissile bond. Six runs with a total of 210 optimization cycles were done. The optimized complex is hereafter noted LM1 ROT. Its final AM1 heat of formation is -1.838 445 au.

(3) Starting from LM1 ROT, all the dihedrals of the NH-C α H-CO backbone were added to the previous 342 variables, leading to 525 unfrozen internal coordinates. The Ser195 side chain remained in the same orientation as in the LM1 ROT optimized structure. Fifteen runs with a total of 500 cycles were

(19) Lamotte-Brasseur, J.; Dive, G.; Dehareng, D.; Ghuyssen, J. M. J. *Theor. Biol.* 1990, 145, 183.

(20) Dewar, M. J. S.; Zoebisch, E. G.; Healy, E. F.; Stewart, J. J. P. *J. Am. Chem. Soc.* 1985, 107, 3902.

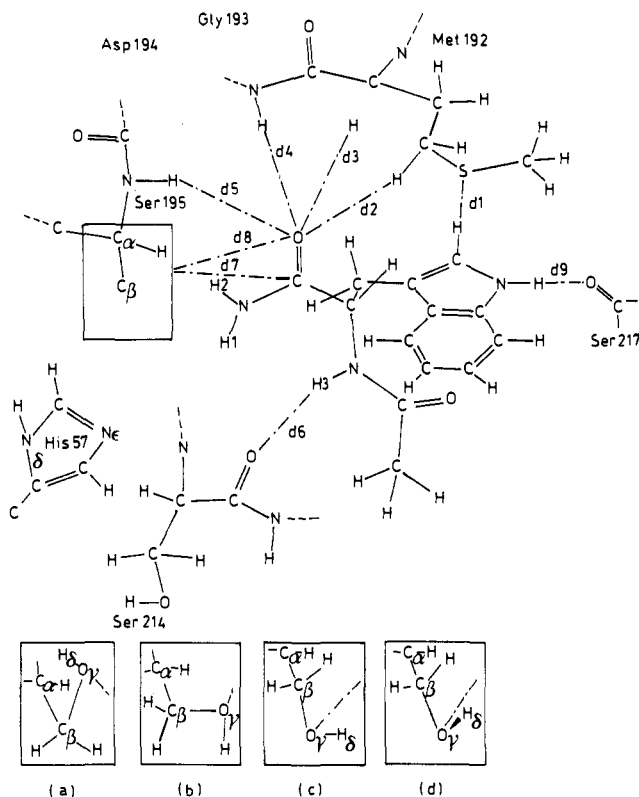


Figure 2. Schematic view of TRYPT in the CHT(23) cavity and definition of the distances used in Table 1. The orientations of the Ser195 side chain correspond to (a) LM1 OPT; (b) LM1 ROT and LM1 ROT-REL1; (c) LM1 ROT-REL2 and LM1r; and (d) LM1 water.

done. The optimized complex is hereafter noted LM1 ROT-REL1. Its final AM1 heat of formation is $-2.026\ 175$ au.

(4) The same 525 internal coordinates as in optimization 3 were chosen as variables. The Ser195 side chain was oriented as in the EL/D11 conformation of ref 21, i.e. the Ser195 O_γ is directed toward His57 whereas its H_β points toward Val213 and Ser214. Nine runs with a total of 270 cycles were done. The optimized complex will be noted LM1 ROT-REL2. Its final AM1 heat of formation is $-2.038\ 349$ au.

(5) The same 525 internal coordinates as in optimization 3 were chosen as variables. Though the Ser195 and His57 side chains were initially oriented as in Wipff's LM1r complex, i.e. the Ser195 H_β and His57 N_ϵ faced each other with a distance of $2.57\ \text{\AA}$, in the optimized conformation the Ser195 H_β has rotated so that it is now the Ser195 O_γ that is oriented toward a hydrogen of the His57 imidazole ring (Figure 2). The distance between the Ser195 H_β and the His57 N_ϵ has become equal to $4.36\ \text{\AA}$. Six runs with a total of 174 cycles were done. The optimized complex will be noted LM1r, as in Wipff's work. Its final AM1 heat of formation is $-2.040\ 124$ au.

The two optimized complexes LM1 ROT-REL2 and LM1r were found to be the same conformation. The intermolecular distances differ from 0.01 to $0.10\ \text{\AA}$ (Table 1), and the energy difference between them is $1.114\ \text{kcal/mol}$. This emphasizes the usefulness of the analytical CNDO electrostatic calculation²¹ that led to EL/D11. The detailed analysis was then performed only on one of them, LM1 ROT-REL2.

Furthermore, a sixth optimization was performed with a water molecule in the active site, between Ser195, His57, Ser214, and TRYPT. To the previous 525 variables were added the nine degrees of freedom related to the introduction of the water molecule. The position and orientation of H_2O were first optimized at the electrostatic CNDO level²¹ in the initial

Table 1. Distances (\AA) between CHT(23) and TRYPT for the Six AM1 Optimized Complexes, According to Figure 2, and for the LM1 Complex Obtained by Wipff et al.¹⁵

d1	d2	d3	d4	d5	d6	d7	d8	d9
LM1 from Wipff et al.								
	1.96	1.76	2.36					2.50
LM1 OPT								
2.543	3.484	2.169	2.289	2.292	2.218	3.113	2.777	2.286
LM1 ROT								
2.472	2.198	2.690	3.617	4.815	2.215	3.061	3.454	2.217
LM1 ROT-REL1								
2.920	2.336	2.220	2.165	3.981	2.916	3.047	3.609	2.187
LM1 ROT-REL2								
2.951	4.002	2.577	2.118	2.216	2.313	3.980	3.834	2.292
LM1r								
2.955	4.100	2.640	2.124	2.204	2.295	3.988	3.803	2.322
LM1 water								
2.948	4.173	2.687	2.152	2.305	3.776	4.046	3.679	2.256

conformation of the LM1r optimization, i.e. the Ser195 H_β and the His57 N_ϵ facing each other. Four runs with a total of 128 cycles were done. The optimized trimer will be noted LM1 water. Its final AM1 heat of formation is $-2.139\ 844$ au.

Some distances between CHT(23) and TRYPT obtained for the six optimized complexes are presented in Table 1, according to Figure 2. In the case of LM1 water, some distances between H_2O and CHT(23) + TRYPT are presented in Table 2 according to Figure 3.

Interaction Energy Analysis

For the four optimized complexes, the interaction energy was calculated for the ten amino acid groups closest to TRYPT, at the AM1 level and at the *ab initio* SCF level, within the MINI-1 and the 6-31G basis sets. Moreover, an energy decomposition according to a Kitaura-Morokuma scheme²² was also performed at the SCF level within the MINI-1 basis set because of its performance in such calculations.²³ These ten groups were not taken as full amino acid residues but had to be truncated in order to fit in with the AMBER program dimensions. They are presented in Figure 4. The interaction energies and the energy components are presented in Tables 3-6. Furthermore, two ways of summing the individual interaction energies are presented in Table 7 for the four complexes. In the SE1 sum, the Gly193 contribution to the interaction comes from its $N-H$ (Figure 2), whereas in SE2, the whole Gly193 is extended to the $C=O$ of Met192 and to the $N-H$ of Asp194. For the four complexes, the cooperativity of the latter fragments results in a greater attractive interaction that emphasizes the influence of the environment around the principal interagents (see below). From Tables 3-5, at the view of columns Gly193, Met192ch, and Met192chGly193, E(EX) and E(CT) are additive components, E(PL) does not seem to be additive but it is small, and E(ES) is not at all additive. This kind of feature has already been pointed out in the case of smaller complexes.²³ From Tables 3-6, in the case of the two backbone-restrained complexes LM1 OPT and LM1 ROT, the Ser190 to Ser189 amino acids destabilize the complex whereas they contribute to the LM1 ROT-REL1 and ROT-REL2 stabilizations.

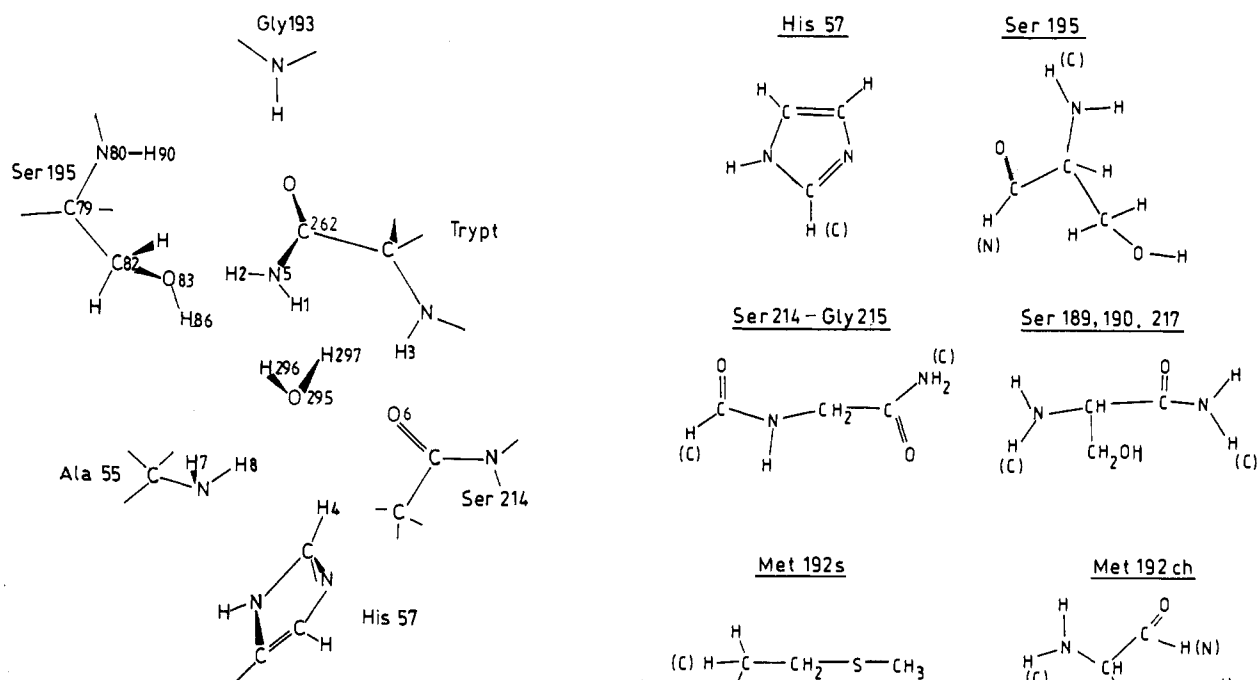
In order to further investigate the kind of tweezer constituted of Gly196 to Val213 around the TRYPT, energy calculations were performed at the semiempirical AM1 and *ab initio* SCF levels within the MINI-1 basis set, for three subgroups of the whole complex. The first group extends from Met192 to Gly196 (57 atoms, 181 AO), the second group is composed of Ser189 to

(22) Kitaura, K.; Morokuma, K. *Int. J. Quantum Chem.* 1976, 10, 325.

(23) Dive, G.; Dehareng, D.; Ghuysen, J. M. *Theor. Chim. Acta* 1993, 85, 409.

Table 2. Distances (Å) between the Water Atoms and the CHT(23) + TRYPT Atoms in the LM1 Water Complex, According to Figure 3

O295-O6	O295-H3	O295-H7	O295-H8	O295-H86	O295-H4	H296-O83	H296-N5	H297-O6	H297-C262
2.851	2.266	2.287	2.484	2.281	2.264	2.700	3.036	2.224	3.888

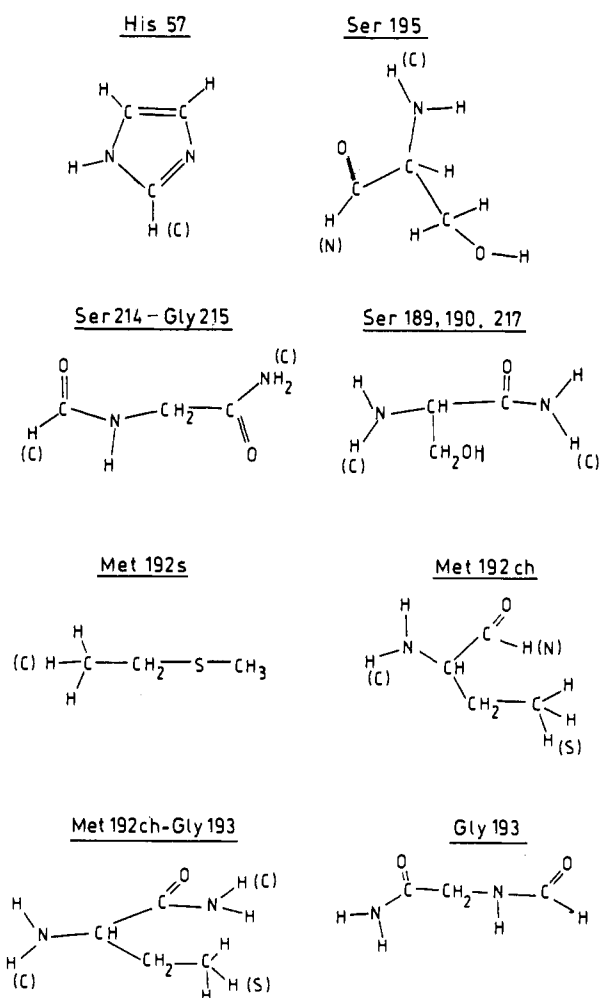
**Figure 3.** Schematic view of H₂O in the complex LM1 water.

Gly196 (86 atoms, 274 AO) and the third group contains from Ser214 to Cys220 (81 atoms, 257 AO). The interaction energies of TRYPT with these groups and with the whole active site model are presented in Table 8.

For the LM1 OPT and ROT complexes, the interaction with TRYPT is unfavorable with the Gly196 to Met192 and Gly196 to Ser189 groups whereas it is attractive with the Ser214 to Cys220 group. When the backbone is relaxed, i.e. considering the LM1 ROT-REL1 and ROT-REL2 complexes, this latter part of the interaction energy does not vary significantly whereas that related with the Gly196 to Ser189 group becomes largely predominant. According to Tables 5 and 6, every amino acid of the group contributes to this interaction energy at a similar level.

When going from LM1 OPT to LM1 ROT, the Ser195 side chain is rotated so that its O_γ is able to attack the carbon of the TRYPT carbonyl. This leads to a less attractive interaction energy and even to a repulsive component with the Ser195-containing groups, though the total heat of formation for the LM1 ROT complex is about 0.78 kcal/mol lower than the LM1 OPT one. This unfavorable interaction with Ser195 is also found in LM1 ROT-REL1, in particular by comparison with LM1 ROT-REL2. For LM1 ROT and LM1 ROT-REL1, characterized by the same orientation of the Ser195 side chain, the interaction energies (AM1 and *ab initio*) of Ser195 with TRYPT are positive, except for the case of LM1 ROT-REL1 in AM1 where it is very small.

In LM1 water, the interaction between TRYPT and CHT(23) is significantly lowered (Table 8) by reference to LM1 ROT-REL2: the interaction energy lost is about 3 kcal/mol for TRYPT with the sum (Gly196 → Ser189) + (Ser214 → Cys220) and about 6 kcal/mol for the case with the whole active site model. The 3 kcal/mol difference comes mainly from the loss of interaction with His57 (Table 6) in relation with the distance changes shown in Table 9. However, if one considers the interaction between the CHT(23) and the dimer TRYPT + H₂O (TW in Table 8), the energy components are very similar to those in LM1 ROT-REL2. The loss of interaction of CHT(23) with TRYPT is compensated by an interaction gain with H₂O, namely via Ser195, Ser214, and a little His57 (Table 2).

**Figure 4.** Ten molecules used to estimate the individual interactions between TRYPT and the CHT(23) closest residues. These ten molecules are noted as the residues they represent. The Met192 residue was truncated into two parts: the first one only involves the side chain with its sulfur atom (Met192s); the second does not consider the side chain sulfur (Met192ch). This second part is either associated (Met192-chGly) or not associated with the Gly193 NH group.

Nature of the Interaction

From Tables 3–5, the smaller components $E(PL)$ and $E(CT)$ do not vary very much from one interaction to the other. This is not the case for $E(1)$ and its components $E(ES)$ and $E(EX)$, whose variations are about 6 kcal/mol. Furthermore, the variation of the interaction energy INT does not follow that of any of the energy components, each participating at a similar level to the interaction. $E(ES)$ and $E(EX)$ are significantly higher than $E(PL)$ and $E(CT)$, but they have opposite signs, resulting in a $E(1)$ of a few kcal/mol, as is the case for $E(PL)$ and $E(CT)$. Moreover, it is known²³ that MINI-1 overestimates $E(CT)$ and underestimates $E(ES)$ and $E(PL)$. $E(PL)$ and $E(CT)$ are by essence stabilizing components, but $E(1)$ can be either stabilizing or destabilizing. In nearly all the cases, it is a little greater than $E(CT)$ in absolute value and $E(PL)$ is the smaller component.

Thus, the overall interaction cannot be reduced to one highly predominant component. Short-range interactions $E(EX)$ and $E(CT)$ of a quantum-mechanical origin, as well as long-range ones of classical meaning $E(ES)$ and $E(PL)$, equally play a role in the stability of the complex.

Table 3. Energy Components within MINI-1 and Interaction Energies within MINI-1, 6-31G, and AM1 between TRYPT and the Ten Chosen Groups (See Text), in the Case of the LM1 OPT Complex^a

energy component	His57	Ser195	Ser214-Gly215	Ser217	Gly193	Ser189	Ser190	Met192chGly	Met192ch	Met192s
ES	-2.543	-4.052	-5.981	-4.613	-4.775	-0.246	-2.389	-4.341	-2.330	-1.979
EX	+1.147	+7.305	+8.227	+5.504	+1.458	+1.061	+8.256	+7.593	+6.059	+4.125
<i>E</i> (1)	-1.396	+3.253	+2.246	+0.891	-3.317	+0.815	+5.867	+3.252	+3.729	+2.146
PL	-0.208	-0.395	-0.767	-0.376	-0.337	-0.047	-0.424	-0.324	-0.707	-0.141
CT	-0.531	-2.908	-3.058	-1.922	-1.596	-0.430	-1.865	-3.638	-2.271	-1.150
Res	+0.041	+0.097	+0.120	+0.049	-0.007	+0.047	+0.153	+0.121	+0.137	+0.142
INT(MINI-1)	-2.094	+0.046	-1.458	-1.359	-5.257	+0.385	+3.731	-0.590	+0.889	+0.998
INT(6-31G)	-4.149	-0.528	-4.252	-1.327	-8.545	+0.248	+3.405	-2.092	+1.452	+1.423
INT(AM1)	-2.135	-0.803	-2.952	-2.342	-4.950	-0.273	+1.395	-2.237	+0.003	+0.001

^a The energies are in kcal/mol. The ten groups are noted as the residues they represent (Figure 4). Abbreviations: ES = electrostatic energy; EX = exchange repulsion energy; *E*(1) = ES + EX; PL = polarization energy; CT = charge transfer energy; Res = residual energy; INT = total interaction energy.

Table 4. Energy Components within MINI-1 and Interaction Energies within MINI-1, 6-31G, and AM1 between TRYPT and the Ten Chosen Groups (See Text), in the Case of the LM1 ROT Complex^a

energy component	His57	Ser195	Ser214-Gly215	Ser217	Gly193	Ser189	Ser190	Met192chGly	Met192ch	Met192s
ES	-3.092	+0.424	-5.505	-5.173	-1.204	-0.458	-2.517	-1.469	-1.575	-4.638
EX	+1.516	+4.329	+6.645	+5.001	+0.017	+0.517	+6.855	+5.538	+6.496	+9.012
<i>E</i> (1)	-1.576	+4.753	+1.140	-0.172	-1.187	+0.059	+4.338	-5.069	+4.931	+4.374
PL	-0.240	-0.214	-0.843	-0.425	-0.087	-0.047	-0.311	-0.236	-0.213	-0.300
CT	-0.385	-0.946	-2.619	-2.122	-0.007	-0.167	-1.468	-2.073	-2.081	-2.616
Res	+0.020	+0.086	+0.088	+0.032	-0.017	+0.011	+0.151	+0.133	+0.149	+0.144
INT(MINI-1)	-2.182	+3.678	-2.234	-2.688	-1.297	-0.145	+2.711	+2.893	+1.297	+1.604
INT(6-31G)	-3.401	+4.993	-5.056	-2.918	-2.528	-0.217	+2.338	+3.027	+2.902	+1.900
INT(AM1)	-2.456	+1.159	-2.797	-3.189	-1.541	-0.428	+0.441	+0.143	+0.065	-1.080

^a See footnote a of Table 3.

Table 5. Energy Components within MINI-1 and Interaction Energies within MINI-1, 6-31G, and AM1 between TRYPT and the Ten Chosen Groups (See Text), in the Case of the LM1 ROT-REL1 Complex^a

energy component	His57	Ser195	Ser214-Gly215	Ser217	Gly193	Ser189	Ser190	Met192chGly	Met192ch	Met192s
ES	-4.275	-0.792	-5.580	-5.297	-5.467	-1.668	-4.176	-5.616	-1.706	-2.216
EX	+1.242	+2.975	+6.507	+6.796	+2.159	+2.298	+4.264	+7.128	+4.954	+2.653
<i>E</i> (1)	-3.033	+2.183	+0.927	+1.499	-3.308	+0.630	+0.088	+1.512	+3.248	+0.437
PL	-0.377	-0.183	-0.522	-0.482	-0.444	-0.078	-0.273	-0.601	-0.381	-0.239
CT	-1.045	-0.564	-2.061	-2.772	-1.872	-1.065	-1.223	-3.827	-2.207	-1.428
Res	+0.006	+0.078	+0.100	+0.097	+0.004	+0.074	+0.055	+0.062	+0.088	+0.056
INT(MINI-1)	-4.449	+1.513	-1.557	-1.658	-5.627	-0.439	-1.353	-2.854	+0.749	-1.174
INT(6-31G)	-7.887	+1.190	-4.863	-2.051	-9.705	-1.182	-3.133	-5.396	-1.770	-2.090
INT(AM1)	-3.090	-0.191	-2.825	-3.573	-5.184	-1.360	-2.359	-3.635	-1.444	-1.073

^a See footnote a of Table 3.

Table 6. Interaction Energies within MINI-1, 6-31G, and AM1 between TRYPT and the Ten Chosen Groups (See Text), in the Case of the LM1 ROT-REL2 Complex^a

energy component	His57	Ser195	Ser214-Gly215	Ser217	Gly193	Ser189	Ser190	Met192chGly	Met192ch	Met192s
INT(MINI-1)	-1.274	-2.817	-1.735	-1.906	-4.836	-0.280	-1.584	-2.770	+0.057	-0.721
INT(6-31G)	-4.186	-5.105	-5.193	-2.426	-7.709	-1.197	-3.278	-5.651	-1.786	-1.302
INT(AM1)	-2.717	-3.329	-3.093	-3.757	-4.256	-0.324	-2.533	-4.531	-1.925	-1.201

^a See footnote a of Table 3.

Table 7. Sum of the Individual Interaction Energies (kcal/mol) from Tables 3-6^a

complex	AM1		MINI-1		6-31G	
	SE1	SE2	SE1	SE2	SE1	SE2
LM1 OPT	-9.346	-12.056	-0.341	-4.119	-7.272	-12.273
LM1 ROT	-8.207	-9.826	+3.637	+2.223	+0.666	-1.987
LM1 ROT-REL1	-18.106	-21.099	-11.970	-13.993	-25.412	-31.491
LM1 ROT-REL2	-21.485	-23.135	-13.087	-15.096	-28.338	-32.183

^a SE1 = His57 + Ser195 + Ser214-Gly215 + Ser217 + Ser189 + Ser190 + Met192chGly193 + Met192s. SE2 = His57 + Ser195 + Ser214-Gly215 + Ser217 + Ser189 + Ser190 + Gly193 + Met192ch + Met192s.

Environment Effect

Two models were constructed in which TRYPT was replaced by the formamide and its interacting partner (IP) by a model amino acid series. The conformation of the amino acids was that of LM1 OPT, and the calculations were performed at the *ab initio* SCF level with the MINI-1 basis set. Two regions of the

active site were chosen to construct the two IP's, according to the proximity of the H₂N-CO-TRYPT fragment. The first one (IP1-*i*) consists of the Gly193-Met192 group with its direct environment Asp194, Cys191, and Ser190 that are not inside the active site and thus do not directly interact with TRYPT. The second one (IP2-*i*) is composed of the His57 residue with its direct environment Ala56, Ala55, and Cys58 that, again, are not inside the active site. The models are constructed as follows.

In the IP1-*i*'s, the SCH₃ group of Met192 is replaced by a OH function: IP1-1 = Gly193-Met192; IP1-2 = Gly193-Met192-Cys191, where the bisulfide bridge connecting it to Cys220 is replaced by a OH function; IP1-3 = Gly193-Met192-Cys191-Ser190; IP1-4 = Asp194-Gly193-Met192-Cys191, where Asp194 is reduced to NH-C_αH₃; IP2-1 = His57 alone; IP2-2 = Ala56-His57; IP2-3 = Ala55-Ala56-His57; IP2-4 = Cys58-His57-Ala56, where the bisulfide bridge with Cys42 is replaced by a OH group. The energy components are presented in Table 10.

For every case, all the components remain quasi constant except the electrostatic one. For the nearest group IP1-*i*, it can vary by

Table 8. Interaction Energies between TRYPT and Three Groups of Residues (See Text), versus the Calculation Level, for the Five CHT(23) + TRYPT Complexes^a

calculation level	Gly196 → Met192	Gly196 → Ser189	Ser214 → Cys220	AS
LM1 OPT				
SCF/MINI-1	-3.246	+2.555	-1.598	
semiempirical/AM1	-5.880	-1.880	-5.101	-9.262
LM1 ROT				
SCF/MINI-1	+5.115	+7.500	-3.544	
semiempirical/AM1	-0.519	-0.344	-5.263	-7.406
LM1 ROT-REL1				
SCF/MINI-1	-4.345	-7.276	-3.217	
semiempirical/AM1	-6.206	-9.638	-6.364	-20.381
LM1 ROT-REL2				
SCF/MINI-1	-10.261	-10.792	-3.703	
semiempirical/AM1	-11.345	-12.238	-6.727	-25.001
LM1 water (T)				
semiempirical/AM1	-9.964	-10.822	-5.026	-18.826
LM1 water (TW)				
semiempirical/AM1	-10.905	-11.766	-6.233	-25.008

^a AS = whole active site model with its 23 amino acids. The energies are in kcal/mol. For LM1 water, the interaction with the three groups of residues if considered for TRYPT alone (T) and the dimer TRYPT + H₂O (TW).

Table 9. Distances (Å) between the His57 N_ε and Three Hydrogens of TRYPT in Four Complexes According to Figure 2^a

complex	r1	r2	r3
LM1 ROT-REL1	2.612	4.089	2.893
LM1 ROT-REL2	2.803	3.709	2.939
LM1 water	4.868	5.808	4.455
LM1 from Wipff ¹⁵	5.270	5.040	4.530

^a r1 = N_ε-H1; r2 = N_ε-H2; r3 = N_ε-H3.

ca. 1.5 kcal/mol as well as the total interaction energy. This clearly points out the long-range tail effect of the electrostatic component of the direct environment. If one remembers that the interactions can happen with the whole molecule of tryptophanamide (namely four N-H...X possible interactions and two CO...X' ones), the active site residues' direct environment energetic effect can extend to several kcal/mol.

For the second series of partners IP2-*i*, the energy components are very similar from one environment to the other and are small. The smaller distance from His57 to the TRYPT formamide is 4 Å and implies the His57 N_ε. It thus seems that the neighbors have nearly no influence on the interactive properties of this part of His57. Furthermore, such long distances lead to much smaller interactions than are presented in Table 3. This is due to the fact that, for LM1 OPT, His57 is mostly in interaction with the hydrogen of the H-N-acetyl (HNAc) chain of TRYPT, the distance between this H and His57 N_ε being 2.55 Å.

Deformation Energy

The deformation energies of TRYPT in the complexes are calculated at the semiempirical AM1 and *ab initio* SCF MINI-1 levels as follows: DE(X) = E_X (studied conformation) - E_X (X optimized conformation) X = AM1, MINI-1. The TRYPT AM1 (TRYPT//AM1) and MINI-1 (TRYPT//MINI-1) optimized conformations are very similar geometrically. The results are presented in Table 11.

The high values obtained in MINI-1 for the RTP column come from the fact that the optimized distances in AM1 and MINI-1 are different and the energy is more sensitive to the distance variation than to the angular one. In fact, as referred to the TRYPT//AM1 conformation, the AM1 energy difference of the TRYPT//MINI-1 conformation is 23.325 kcal/mol while it decreases to 5.518 kcal/mol for a conformation where the distances come from the TRYPT//AM1 and the angles and dihedrals

come from the TRYPT//MINI-1. This quantity becomes equal to 2.494 kcal/mol for the conformation where the distances and the angles come from the TRYPT//AM1 and the dihedrals come from the TRYPT//MINI-1. Thus, the variation of the conformational energy related to the calculation level lies around 2.5 kcal/mol. Consequently, the MINI-1 deformation energies in Table 11 are higher than the AM1 ones.

The deformation of TRYPT is far from being negligible at the two geometric and energetic points of view. Geometrically (Figure 5), the TRYPT deformation in LM1 OPT is the most important; it is somewhat smaller in LM1 ROT, very similar to that in LM1 ROT-REL1, and finally smaller in LM1 ROT-REL2 and in LM1 water. At the AM1 level, the related deformation energy ranges from 5 to 10 kcal/mol except for LM1 water, where it drops down to about 3 kcal/mol. This decrease could be linked to an opening of the cavity in the environment of H₂O and thus to a least influence of the enzyme on TRYPT in this region. This can be related to the decrease of the interaction energy between TRYPT and CHT(23) (Table 8). At the *ab initio* MINI-1 level, apart from LM1 OPT, the variation of the deformation energy for the different complexes is very similar to that in AM1. However, the absolute values are higher. It is not very surprising, since, in many cases, AM1 provides conformational energy surfaces that are too flat compared with *ab initio* results.

Relaxation of the Backbone

The effect of the backbone relaxation can be discussed on the basis of the differences between LM1 ROT and LM1 ROT-REL1.

Considering first the geometry (Table 1), the relaxation of the backbone allows the TRYPT to better position its carbonyl oxygen in the oxyanion hole, as seen by the considerable decrease of *d*₃, *d*₄, and *d*₅, while the attack orientation of the Ser195 O_γ does not change significantly (*d*₇ and *d*₈). Moreover, the distance to the carbonyl oxygen of the Ser214 (*d*₆) increases. This can be related to the fact that the Ser195 H_δ is oriented so as to also interact with this Ser214 oxygen carbonyl, the related distance passing from 3.134 Å in LM1 ROT to 2.110 Å in LM1 ROT-REL1, and thus to decrease the Ser214 C=O influence on the side chain of TRYPT. The motion of Ser214 is linked to that of Asp102 (cf. the variation of the distance between the Ser214 H_δ and the free oxygen of the Asp102 side chain from 3.167 Å in LM1 ROT to 2.205 Å in LM1 ROT-REL1), which is in turn linked to His57 motion (cf. the variation of the distance between the hydrogen of the His57 N_δ-H and the free oxygen of the Asp102 side chain from 2.575 Å in LM1 ROT to 2.291 Å in LM1 ROT-REL1). The observed result is that the distance between the His57 N_ε and the Ser195 H_δ passes from 2.499 Å in LM1 ROT to 4.131 Å in LM1 ROT-REL1. Moreover, the backbone relaxation opens the oxyanion hole, i.e. the distance between the two involved hydrogens passes from 2.619 Å in LM1 ROT to 3.411 Å in LM1 ROT-REL1.

Furthermore, it is worth remarking that the 23 amino acids of LM1 OPT and LM1 ROT are nearly superimposed except for the Ser195 side chain, but this is not at all true for LM1 ROT-REL1 and LM1 ROT-REL2, as reflected for instance in Table 12.

From the energetic point of view, the destabilizing groups in LM1 ROT, i.e. Met192ch, Met192s, Ser195, and Ser190, become either much less repulsive (Ser195) or attractive in LM1 ROT-REL1 (Tables 4 and 5). Nevertheless, the already stabilizing groups Ser214-Gly215 and Ser217 do not become more attractive in LM1 ROT-REL1 (Tables 4, 5, and 8). These observations are independent of the calculation level. This clearly indicates that the molecular mechanics energy optimization leads to a too compact ligand-active site complex. This is the first time that such a qualitative calibration of the molecular mechanics results

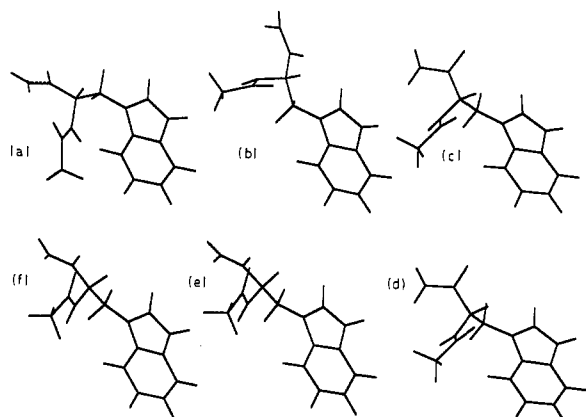
Table 10. Energy Components (kcal/mol) for the Two IP Models (See Text) with the Tryptophanamide Represented by the Formamide, within the MINI-1 Basis Set^a

energy component	Fo + IP1-1	Fo + IP1-2	Fo + IP1-3	Fo + IP1-4	Fo + IP2-1	Fo + IP2-2	Fo + IP2-3	Fo + IP2-4
ES	-4.924	-3.320	-4.002	-3.673	-1.099	-1.065	-0.9977	-0.944
EX	+6.705	+6.474	+6.445	+6.454	+0.004	+0.005	+0.0002	+0.011
E(1)	+1.781	+3.154	+2.443	+2.781	-1.095	-1.060	-0.9975	-0.933
PL	-0.309	-0.262	-0.316	-0.290	-0.038	-0.036	-0.039	-0.030
CT	-3.410	-3.452	-3.515	-3.486	-0.007	-0.006	-0.015	+0.007
Res	+0.150	+0.135	+0.177	+0.152	+0.004	+0.002	+0.016	-0.018
INT	-1.788	-0.425	-1.212	-0.843	-1.137	-1.100	-1.036	-0.974

^a Fo = formamide.**Table 11.** Deformation Energies (kcal/mol) of TRYPT in the Five AM1 Optimized Complexes at the Semiempirical AM1 and *ab initio* SCF MINI-1 Levels^a

complex	AM1			MINI-1		
	P	TP	RTP	P	TP	RTP
LM1 OPT	10.300	8.584	8.455	7.477	9.260	25.766
LM1 ROT	8.015	6.146	6.123	11.277	11.874	29.865
LM1 ROT-REL1	9.505	6.583	6.689	12.433	11.852	28.957
LM1 ROT-REL2	6.406	4.653	4.957	11.827	9.418	25.722
LM1 water	5.173	3.185	3.362	10.495	8.243	24.492

^a Abbreviations: RTP = distances, angles, and dihedrals of TRYPT in the complex; TP = angles and dihedrals of TRYPT in the complex, distances from the TRYPT AM1 or MINI-1 optimized conformation; P = dihedrals of TRYPT in the complex, distances and angles from the TRYPT AM1 or MINI-1 optimized conformation.

**Figure 5.** TRYPT conformation: (a) AM1 optimized conformation; (b) TRYPT in the LM1 OPT conformation; (c) TRYPT in the LM1 ROT conformation; (d) TRYPT in the LM1 ROT-REL1 conformation; (e) TRYPT in the LM1 ROT-REL2 conformation; (f) TRYPT in the LM1 water conformation.**Table 12.** Distances (Å) for Three Complexes between H2 (Figure 2) and the Nitrogen of the Cys42 Terminal NH₂ and between H2 and the Sulfur of the Cys42 Side Chain

complex	distance H2- -N(Cys42)	distance H2- -S(Cys42)
LM1 ROT-REL1	4.842	4.031
LM1 ROT-REL2	2.676	3.188
LM1 water	2.574	3.367

on an active site–ligand system is made versus the more sophisticated quantum mechanical calculations.

A considerable interaction energy gain is observed when the backbone can relax. Considering Table 8, the AM1 interaction energy change is about -13 kcal/mol from LM1 ROT to LM1 ROT-REL1. When reduced to the sum of the interactions with the two groups Gly196 → Ser189 and Ser214 → Cys220, this change is about -10 kcal/mol in AM1 and -14 kcal/mol in MINI-1. These values are similar to those deduced from Table 7 for SE1 and SE2 and range from -26 to -29 kcal/mol in 6-31G. This great interaction improvement by the backbone relaxation is accompanied by a huge geometrical relaxation energy, since the total AM1 energy change is -117.8 kcal/mol.

Position and Freedom of the Water Molecule

The water molecule is well positioned to play the role of a proton transmitter from Ser195 to the leaving NH₂ TRYPT moiety in a concerted hydrolysis mechanism: the distance between the water oxygen and the Ser195 H_δ is about 2.3 Å (Table 2), that between one of the water hydrogens and the nitrogen of the leaving TRYPT NH₂ is about 3 Å, whereas the distance between the Ser195 O_γ and the carbon of the TRYPT carbonyl lies around 4 Å. Furthermore, the oxygen of the Ser214 carbonyl interacts with the second water hydrogen, and the water oxygen lies near several stabilizing groups. The interaction energy of H₂O with the dimer CHT(23) + TRYPT is -8.940 kcal/mol, and that with TRYPT alone is -2.759 kcal/mol.

This idea that the hydrolysis could be a concerted instead of a two-step mechanism has already been proposed by Dive *et al.* in an *ab initio* level study.⁹ This topic is the subject of a proximate publication²⁴ of ours.

In a recent work²³ on small H-bonded complexes, it has been shown that the motion of the water molecule in the methanol–water–imidazole trimer needed not much energy: for 1 or 2 kcal/mol, the amplitude of its motion was not at all negligible. The study was presented in MINI-1, but AM1 calculations were also made,²⁵ indicating that AM1 amplitudes were roughly twice too large compared with *ab initio* SCF MINI-1 ones.

An AM1 energy scan was run with the six water relative degrees of freedom as variables for the LM1 water complex. The results are presented in Table 13 according to Figure 3. Even if the obtained AM1 amplitudes should be approximately divided by 2 for comparison with *ab initio* results, the water motion still does not need much energy. This can be related to Nakagawa *et al.*'s molecular mechanical results,¹¹ emphasizing namely the mobility of the water molecules in the reaction region of the acylchymotrypsin.

Quantum Chemical Results versus Molecular Mechanics Ones

Our results are compared with those of Wipff *et al.*¹⁵ These authors do not find any interaction with the His57 group (their group 2) whereas the most important interactions are with the Gly196 → Ser189 and Val213 → Thr222 groups (Table III of ref 15). This can be related to the distances reported here in Tables 1 and 9.

The predominant energy component was the van der Waals (vdW) term, much greater than the electrostatic one. The attractive 1/*r*⁶ vdW component can be related to the long-range dispersion term of classical mechanics, which is often on the same order of magnitude as the classical induction term PL when the intersystem distances are on the order of 2 Å,²³ i.e. much lower than the electrostatic one for polar interacting partners. From the view of our discussion about the backbone relaxation, the too compact complexes obtained by molecular mechanics could be related with a possible overestimation of the vdW term and underestimation of the electrostatic one probably linked partly to the screening by the dielectric constant.

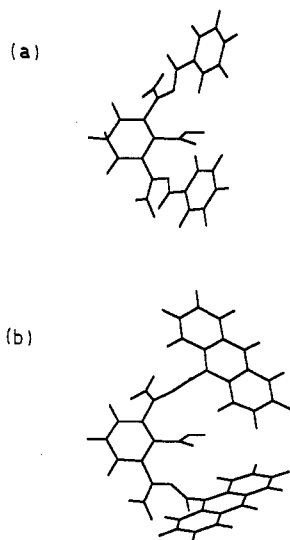
(24) Dive, G.; Dehareng, D. In preparation.

(25) Unpublished results, available on request.

Table 13. Minimal and Maximal Values of the Six Parameters Defining the Water Position in LM1 Water Related to Two Energy Variations, Corresponding to Figure 3^a

scan of r_{294} (Å)			scan of t_{293} (deg)			scan of t_{294} (deg)			scan of p_{292} (deg)			scan of p_{293} (deg)			scan of p_{294} (deg)		
E	r_{294}	Δr_{294}	E	t_{293}	Δt_{293}	E	t_{294}	Δt_{294}	E	p_{292}	Δp_{292}	E	p_{293}	Δp_{293}	E	p_{294}	Δp_{294}
1.0	-0.17	0.38	1.0	-2.50	3.5	1.0	-15.0	29.0	1.0	-12.0	20.0	1.0	-20.0	36.0	1.0	-17.0	44.0
	+0.21			+1.00			+14.0			+8.0			+16.0			+27.0	
2.0	-0.24	0.54	2.0	-5.50	8.0	2.0	-22.0	43.0	2.0	-17.0	28.0	2.0	-27.0	53.0	2.0	-25.0	62.0
	+0.30			+2.50			+21.0			+11.0			+25.0			+37.0	

^a The energies are in kcal/mol. r_{294} = distance O295-H86; t_{293} = valence angle O295-H86-C82; t_{294} = valence angle H296-O295-H86; p_{292} = dihedral O295-H86-C82-O83; p_{293} = dihedral H296-O295-H86-O83; p_{294} = dihedral H297-O295-H296-H86.

**Figure 6.** Schematic representation of two reduced models of Blake and Jorgensen's molecular tweezer (81 atoms): (a) 49 atom model, T1; (b) 73 atom model, T2.

The geometrical differences between our LM1 OPT and the Wipff *et al.*'s LM1 are the following. The side chains of Met192 and His57 as well as the H₃ of Ser195 and Ser214 have rotated significantly, and the TRYPT has moved into the cavity. The oxyanion hole distances, 0.2 Å different in Wipff *et al.*'s results, are quite similar in our LM1 OPT (Table 1). They become 0.1 Å different in our LM1 ROT-REL2 but with the opposite sign.

Though Wipff *et al.* considered that their 2.36-Å distance d_6 (Figure 2) was too high for an interaction to take place, we found similar values for the complexes without water and a non-negligible interaction energy (Tables 3–6). This seems in contradistinction with experimental works that showed that the NHAc chain of TRYPT has no influence on the formation of the Michaelis complex.^{26,27} However, the LM1 water conformation agrees with this observation, since the distance between the NHAc of TRYPT and Ser214 has increased up to 3.776 Å (Table 1) in agreement with the 1.7 kcal/mol interaction energy decrease for the Ser214 → Cys220 group between LM1 ROT-REL2 and LM1 water (T) (Table 8).

Conclusions

The aim of our work on the CHT(23) + TRYPT complex was to study several aspects of the interaction and the deformation of a molecule inside another one. Moreover, this complex was chosen to compare our quantum chemical semiempirical results with those obtained by Wipff *et al.*¹⁵ at the molecular mechanics level. This is the first time that a quantum versus classical comparison is made on such a large molecular system.

The usefulness of a preliminary optimization of the relative

degrees of freedom of the complex at the electrostatic CNDO level²¹ is emphasized from the results of LM1 ROT-REL2 and LM1 water.

When the Ser195 side chain is oriented so that its O_γ points toward the carbonyl carbon of TRYPT to simulate the nucleophilic attack, the interaction Ser195-TRYPT is repulsive (Tables 4 and 5), resulting in an optimized conformation where the carbonyl oxygen of the ligand is no longer in the oxyanion hole.

From the view of the individual residue interaction energies (Tables 3–6), several amino acids contribute to the complex stabilization at the same level (His57, Ser214, and Ser217 for the four complexes; Ser189 and Met192 for LM1 ROT-REL1; Ser190 and Met192 for LM1 ROT-REL2). However, the reduction of the interaction to individual components is only a qualitative tool, since it does not take into account the influence of the environment, which can be non-negligible (Table 10), mainly through its electrostatic properties.

The deformation energy of the TRYPT ligand due to the complex formation varies from one complex to the other, the smaller being for the LM1 water. This can be explained by an opening of the cavity due to the presence of the water molecule and thus to a smaller interaction with TRYPT inducing a smaller deformation. Nevertheless, the conformational deformation energy ranges from 5 to 10 kcal/mol at the AM1 level (Table 11), and from 8 to 12 kcal/mol at the *ab initio* MINI-1 level, which is quite non-negligible.

The backbone relaxation allows the destabilizing groups in LM1 ROT to become either much less repulsive (Ser195) or attractive in LM1 ROT-REL1 (Tables 4, 5, 7, and 8). This is observed at three calculation levels. This implies that the molecular mechanics energy optimization leads to a too compact ligand-active site complex. A considerable interaction energy gain is observed when the backbone can relax (Tables 7 and 8). This great interaction improvement by the backbone relaxation is accompanied by a huge geometrical relaxation energy, since the total AM1 energy change is -117.8 kcal/mol.

A decrease of the interaction energy between CHT(23) and TRYPT is observed in the LM1 water complex (Table 8). The presence of the water molecule eliminates the interaction of TRYPT with Ser214 (increase of d_6 in Table 1) and with His57 (Table 9). This fact could explain why experimentally the presence or the absence of the HNAC TRYPT chain has no influence on the KM.^{26,27}

The position of the water molecule in LM1 water allows it to act as a proton transmitter from Ser195 to the leaving NH₂ TRYPT group in a one-step mechanism. Though its interaction energy with the CHT(23) + TRYPT dimer is non-negligible (-8.940 kcal/mol), the water motion does not need much energy (Table 13).

The comparison of our quantum chemical results with the molecular mechanical ones by Wipff *et al.* shows that their LM1 complex is too restrained. This may come from a possible overestimation of the vdW terms and an underestimation of the electrostatic one in the molecular mechanics parametrization.

(26) Blow, D. M. *Isr. J. Chem.* 1974, 12, 483.

(27) Kraut, J. *Annu. Rev. Biochem.* 1977, 46, 331.

Acknowledgment. This work was supported in part by the Belgian program on Interuniversity Poles of attraction initiated by the Belgian State, Prime Minister's Office, Science Policy Programming (PAI no. 19), the Fonds de la Recherche Scientifique Médicale (Contract no. 3.4531.92), and a Convention tripartite between the Région wallonne, SmithKline Beecham, U.K., and the University of Liège. G. D. is chercheur qualifié of the Fonds National de la Recherche Scientifique (FNRS, Brussels).

Appendix

A molecular tweezer, whose coordinates were kindly provided to us by Professor Jorgensen,²⁸ was modified into two smaller molecules T1 (49 atoms) and T2 (73 atoms) (Figure 6) and optimized at the AM1 level, within the C_s point group. A full numerical Hessian was calculated for the optimized conformations, and they turned out to be first-order critical points,

(28) Blake, J. F.; Jorgensen, W. L. *J. Am. Chem. Soc.* **1990**, *112*, 7269.

characterized by the negative Hessian eigenvalues of -0.00168 au and -0.06605 au, respectively. The negative Hessian eigenvalue corresponded to the rotation of the acidic group in order to form an intramolecular H-bond with the nitrogens aside. For these optimized first-order critical points, a partial numerical Hessian was calculated by estimating only the force constants of the heavy atoms' dihedrals. In the case of the smaller system T1, five negative Hessian eigenvalues were obtained (-0.50072 , -0.16542 , -0.04313 , -0.02355 , and -0.01982 au) whereas eight negative Hessian eigenvalues were obtained for T2 (-1.54471 , -1.54010 , -0.72609 , -0.48748 , -0.48117 , -0.17974 , -0.06973 , -0.02391 au).

The correct estimation of the off-diagonal force constants related to some variables (the dihedral angles in the examples above), without correctly estimating all the corresponding diagonal elements for the variables they are strongly coupled to (the valence angles in this case), leads to an ill-conditioned Hessian characterized by an unrealistic inertia.